



## Rhodamine B removal from aqueous solutions using loofah sponge and activated carbon prepared from loofah sponge

Zhi-ping Qi<sup>a,b,1</sup>, Qun Liu<sup>a,e,1</sup>, Zhuang-Rui Zhu<sup>c</sup>, Qiang Kong<sup>a,\*</sup>, Qing-Feng Chen<sup>d</sup>,  
Chang-Sheng Zhao<sup>d</sup>, Yu-Zhen Liu<sup>a</sup>, Ming-Sheng Miao<sup>e</sup>, Cong Wang<sup>a,e</sup>

<sup>a</sup>Institute of Environment and Ecology, Shandong Normal University, 88 Wenhua Donglu, Jinan 250014, Shandong, P.R. China, emails: 452952020@qq.com (Z.-p. Qi), 373400619@qq.com (Q. Liu), Tel. +86 531 86182550; Fax: +86 531 86180107; emails: kongqiang0531@hotmail.com (Q. Kong), 75980079@qq.com (Y.-Z. Liu), 939715827@qq.com (C. Wang)

<sup>b</sup>No. 1 Middle School of Ningyang County, 42 Wenhua Road, Tai'an 271400, Shandong, P.R. China

<sup>c</sup>School of Business, Shandong University of Political Science and Law, 63 East Jiefang Road, Jinan 250014, Shandong, P.R. China, email: 641433134@qq.com

<sup>d</sup>Key Laboratory for Applied Technology of Sophisticated Analytical Instruments of Shandong Province, Analysis and Test Center, Shandong Academy of Sciences, Jinan 250014, Shandong, P.R. China, emails: chensdcn@163.com (Q.-F. Chen), 247898387@qq.com (C.-S. Zhao)

<sup>e</sup>College of Life Science, Shandong Normal University, 88 Wenhua Donglu, Jinan 250014, Shandong, P.R. China, email: mingshengmiao@163.com (M.-S. Miao)

Received 16 November 2015; Accepted 3 June 2016

---

### ABSTRACT

Loofah sponge and activated carbon (AC) made from it were used to adsorb rhodamine B (RhB) onto aqueous solutions. Scanning electron microscopy of the two materials revealed they possessed rough surfaces; loofah sponge featured a high surface area of 132.6 m<sup>2</sup>/g, which increased to 842.3 m<sup>2</sup>/g for AC. Fourier transform infrared spectroscopy indicated that the surface of both materials was abundant in O–H, C–H, and C=O groups, which may increase their adsorption capacities. The kinetics, isotherms, and optimum conditions for RhB removal were studied. RhB adsorption by the adsorbents was consistent with pseudo-second-order equations. The adsorption isotherms revealed that the adsorption process of loofah sponge involved multilayer adsorption, while that of AC was monolayer adsorption. The optimal performance of AC (removal ratio of 99.20% and equilibrium adsorption of 191.43 mg/g) was achieved using a temperature of 313 K, AC content of 0.6 mg/L, and initial RhB concentration of 120 mg/L. AC displayed an increased adsorption capacity for RhB compared with that of loofah sponge; the maximum equilibrium adsorption of AC reached 333.33 mg/L, which is 14 times that of loofah sponge. AC derived from loofah sponge is a promising adsorbent for RhB removal from aqueous wastewater.

---

\*Corresponding author.

<sup>1</sup>These authors contributed equally to this work.

Presented at the 8th International Conference on Challenges in Environmental Science & Engineering (CESE-2015) 28 September–2 October 2015, Sydney, Australia

*Keywords:* Rhodamine B; Loofah sponge; Activated carbon; Adsorption; Kinetics; Isotherm; Optimal conditions

---

## 1. Introduction

Dyes have been used for a long time. Early natural dyes were nontoxic and stable, but they have gradually been replaced by synthetic dyes because of their limited availability, low yield, and high cost [1]. Since their first synthesis in the 1850s, synthetic dyes have slowly been popularized by virtue of advantages such as easy use, low cost, high yield, high stability, and abundant varieties [2]. With the large-scale use of dyes, dye wastewater discharge has been increasing rapidly [3]. The textile, leather, paper, and printing industries all produce colored effluents, which may contain many toxic dyes that are stable to biodegradation and oxidizing agents [4]. In China, around 160 million cubic meters of dye wastewater is discharged into the water environment annually. Directly discharging dye wastewater into natural rivers can greatly harm the environment, while obviously affecting the appearance of the water. A decrease in water transparency lowers the photosynthesis of aquatic plants, slowing the growth of animals and plants. Dye wastewater may also damage human health via toxin enrichment in the food chain [5]. Meanwhile, dye wastewater can contain large amounts of organic substances that are rich in phosphorus and nitrogen. Therefore, the discharge of dye wastewater can cause water eutrophication. The degradation of organic substances by micro-organisms consumes a lot of the oxygen in water, therefore affecting fish and other aerobic organisms [6]. In addition, some dyes and their degradation products are highly toxic, and some are teratogenic, carcinogenic, and/or mutagenic [7]. Rhodamine B (RhB) is a water-soluble organic dye that is widely used in fluorescent staining, cosmetic products, food processing, and textiles. RhB can burn eyes and irritate the skin and gastrointestinal and respiratory tracts of humans. Thus, the treatment of dye effluents before their discharge into the receiving water environment is important [4,8].

Dyes are difficult to remove from wastewater because of their complex compositions, high stability, and low biodegradability. Thus, finding an effective way to remove dye contaminants from wastewater has become an urgent issue [9]. Treatment of highly colored wastewater containing hazardous industrial chemicals is a growing need at present. Current dye wastewater treatment methods can be divided into physical-chemical and biological methods, among

which the common methods include adsorption, biological treatment, chemical flocculation, chemical oxidation, and electrochemistry. These methods have been used by numerous researchers to remove organics and inorganics from wastewater, as reviewed elsewhere [10–12]. Adsorption has proved to be an efficient and economical process for decontamination of water samples from dyes using different adsorbents. Ion-exchange fibers, natural minerals (diatomite, bentonite), industrial waste (fly ash, cinders), and activated carbon (AC) are common adsorbent materials [13,14]. The adsorption characteristics of ion-exchange fibers mean there is no loss of adsorbent after regeneration, but these fibers are not suitable for all kinds of dyes. Both cinders and fly ash are excellent adsorbents with a honeycomb structure, but their specific surface area is low, resulting in poor treatment efficiency [15]. In contrast, AC is effective for all kinds of dyes. Therefore, some low-cost agricultural by-products or waste and the AC obtained from these raw materials are attracting interest in biological adsorption research for dye wastewater treatment [16–18].

AC has a large specific surface area and large quantities of pores, allowing it to strongly adsorb toxic substances onto the liquid phase or even gas phase. Therefore, AC obtained from raw plant materials is one of the most commonly used adsorbents in current studies [19]. The raw materials used to prepare AC are generally the substances with a high carbon content and low content of inorganic matter. A common early raw material was wood, but deforestation damages the environment and timber resources are limited. Therefore, wood has been replaced by coal, which is abundant and cheap. As the energy issue becomes increasingly prominent, raw materials for AC that are inexpensive, high performing, and abundant have become desirable [20]. Recently, AC has been prepared from agricultural wastes, such as breadfruit skin, peanut shells, oil palm fiber, corncobs, palm kernel shells, and bamboo stems, as well as peat [21–24]. The plant-derived loofah sponge is an inexpensive, readily available biological material with high void volume and permeability, making it suitable as an adsorbent [25]. The AC produced from loofah sponge may have a high adsorption capacity for dye contaminants, but this has not been investigated previously. Thus, it is important to study the adsorption of representative dye RhB by loofah sponge and AC produced from loofah sponge.

In this paper, loofah sponge and AC prepared from loofah sponge are used as adsorbents to remove RhB dye from aqueous solution. The specific surface area and pore size of these two adsorbents are measured. Kinetic and thermodynamic models of adsorption and applicable adsorption isotherms are determined for these adsorbents. This allows us to identify the mechanisms of RhB adsorption by loofah sponge and AC prepared from loofah sponge. Our work reveals a new method to remove dyes from water using loofah sponge.

## 2. Materials and methods

### 2.1. Material preparation

Loofah sponge (obtained from a local market in Jinan) was cleaned and dried at 100°C for 12 h, and then processed into lengths of about 3–4 mm with a grinder. The minced loofah sponge was placed in a heat-resistance box at 120°C for 12 h. The dried loofah sponge was soaked in an appropriate amount of 85% phosphoric acid in deionized water (1:1, v/v) for 12 h [26]. The ratio of the mass of loofah sponge to solution volume was 1:5 (m/v). The activated loofah sponge was placed in the resistance box and carbonized at 450°C for 1 h. After cooling, the carbonized loofah sponge was washed with distilled water until the pH reached 7. The cleaned AC was dried at 120°C for 12 h, cooled, ground with a mortar and pestle, and then sieved through 150–200 mesh to obtain the desired AC. RhB (SR662601 Tianji, China) stock solution with a concentration of 1,000 mg/L was prepared using distilled water. Other RhB concentrations were obtained by diluting the stock solution with distilled water.

### 2.2. Characterization of adsorbents

The surface structure of the loofah sponge and AC prepared from loofah sponge was observed via scanning electron microscopy (SEM; SUPRA™ 55, Zeiss, Germany). Total specific surface area was determined using the Brunauer–Emmett–Teller (BET) theory. Fourier transform infrared (FTIR) spectroscopy (Fourier-380 FT-IR, America) was used to reveal the adsorption mechanism and explore the influence of adsorption on the functional groups in the loofah sponge and AC.

### 2.3. Adsorption experiments

RhB solutions were diluted to different concentrations and detected at 552 nm using an ultraviolet (UV) spectrophotometer (T6, Xinshiji, Beijing) [27]. The

solution after adsorption was filtered using a filter membrane with a pore size of 0.22 μm, and then its absorbance was measured with the UV spectrophotometer at the maximum absorption wavelength of the dye (552 nm). A standard curve was used to calculate dye concentration. The following equations were used to calculate the removal ratio  $\eta$  and equilibrium adsorption  $Q_e$  of the adsorbents [28]:

$$\eta(\%) = \frac{C_0 - C_e}{C_0} \times 100\% \quad (1)$$

$$Q_e = \frac{(C_0 - C_e)V}{W} \quad (2)$$

where  $C_0$  and  $C_e$  represent the initial dye concentration and the dye concentration at adsorption equilibrium (mg/L), respectively,  $V$  represents the volume of the solution (L), and  $W$  represents the mass of the adsorbent (g).

The pH experiments were conducted in the pH range of 1–14 with phosphoric acid or NaOH solution while other process parameters were kept constant. Loofah sponge (0.2 g) or AC (0.08 g) was added to RhB solution (100 mg/L, 100 mL) in a series of 150-mL Erlenmeyer flasks. The Parafilm-covered flasks were put on a shaker at 180 rpm and 298 K for 3 h to attain equilibrium. The suspensions were filtered through a syringe-driven filter and then the RhB concentrations of the filtrates were measured by absorption spectroscopy.

To determine the effect of adsorbent dose on RhB removal, adsorption experiments were performed at adsorbent doses of 0.4, 0.8, 1.2, 2.0, 2.4, 3.2, and 4.0 g/L for loofah sponge and 0.4, 0.8, 1.0, 1.2, 1.6, and 2.0 g/L for AC. Different adsorbent doses were added to a series of flasks filled with RhB solution (100 mL, 100 mg/L) at natural pH (=4.1). The flasks were agitated on a shaker at 180 rpm and 298 K for 3 h. The sampling and analytical procedures were the same as those described above.

### 2.4. Adsorption kinetics

RhB adsorption kinetics of the loofah sponge and AC were examined by conducting experiments at a given initial RhB concentration of 100 mg/L and specific adsorbent dose of 2.0 g/L for loofah sponge and 0.8 g/L for AC. The pH of the solutions was kept at 1. The adsorption reaction was performed at 180 rpm and 298 K using a thermostatic shaker. At different intervals, aliquots were taken from each solution and filtered. The filtrates were analyzed by absorption spectroscopy to determine RhB concentrations.

#### 2.4.1. Pseudo-first-order equation

The pseudo-first-order equation is widely used to describe the adsorption kinetics of aqueous solutions. Its theoretical basis is that adsorption ratio is affected by solution concentration and adsorption, and the limiting factor of adsorption is the mass transfer resistance within the particles. The equation is written as:

$$\ln(Q_e - Q_t) = \ln Q_e - k_1 t \quad (3)$$

where  $Q_t$  represents the adsorption (mg/g) at time  $t$ , and  $k_1$  represents the pseudo-first-order adsorption ratio constant (1/min). A curve was plotted with  $t$  as the horizontal axis and  $\ln(Q_e - Q_t)$  as the vertical axis, and subjected to linear fitting. The slope of the fitted straight line was used to calculate  $k_1$ , while  $Q_e$  was calculated from the intercept [29].

#### 2.4.2. Pseudo-second-order equation

The pseudo-second-order equation is also widely used to describe the kinetics of adsorption. This equation holds when the adsorption mechanism limits adsorption instead of the mass transfer resistance within particles. The pseudo-second-order equation is written as:

$$\frac{t}{Q_t} = \frac{1}{k_2 Q_e^2} + \frac{1}{Q_e} t \quad (4)$$

and

$$V_0 = k_2 Q_e^2 \quad (5)$$

In these equations,  $V_0$  represents the initial adsorption ratio (mg/(g min)), and  $k_2$  represents the pseudo-second-order adsorption ratio constant (g/(mg min)). A curve was plotted with  $t$  as the horizontal axis and  $t/Q_t$  as the vertical axis and was also subjected to linear fitting. The values of  $Q_e$ ,  $k_2$ , and  $V_0$  were calculated from the plot of  $t/Q_t$  vs.  $t$  [30].

#### 2.4.3. Particle diffusion equation

Internal diffusion controls the adsorption ratio in many adsorption processes. We can confirm the type of control process using the particle diffusion equation, which is expressed as follows:

$$Q_t = k_p t^{1/2} + C \quad (6)$$

where  $k_p$  represents the ratio constant of particle diffusion equation (mg/g min<sup>1/2</sup>), and  $C$  represents the intercept, which reflects the thickness of the boundary layer; i.e. the smaller  $C$  is, the less influence the boundary layer will have on adsorption. A curve was plotted with  $t^{1/2}$  as the horizontal axis and  $Q_t$  as the vertical axis and subjected to linear fitting. The values of  $k_p$  and  $C$  were calculated from the slope and intercept of the fitted line, respectively. When the fitted line passes through the origin (i.e.  $C = 0$ ), it indicates that the only factor controlling the adsorption ratio is the internal diffusion process [31].

#### 2.5. Adsorption isotherms

Adsorption isotherm data were obtained as follows. Loofah sponge (0.2 g) or AC (0.08 g) was added to RhB solution (100 mL) with a concentration of 5, 10, 20, 50, or 100 mg/L for loofah sponge and 5, 10, 20, 50, 100, or 200 mg/L for AC in a series of conical flasks. The initial pH values of the suspensions were 1. The suspensions were shaken at 180 rpm and 298 K for 90 min in a thermostatic shaker to ensure that equilibrium was reached. After filtration, the filtrates were analyzed to determine RhB concentrations. Adsorption isotherm data were fitted to Langmuir, Freundlich, and Dubinin–Radushkevich (D–R) models.

##### 2.5.1. Langmuir isotherm equation

The Langmuir isotherm equation is mainly used to describe monolayer adsorption. The general and linear expressions are, respectively, shown as:

$$Q_e = \frac{Q_m K_L C_e}{1 + K_L C_e} \quad (7)$$

$$\frac{C_e}{Q_e} = \frac{1}{Q_m K_L} + \frac{1}{Q_m} C_e \quad (8)$$

where  $K_L$  represents the Langmuir constant (L/mg), which reflects the adsorption ratio, and  $Q_m$  represents the maximum adsorption capacity of adsorbent (mg/g). A curve was plotted with  $C_e$  as the horizontal axis and  $C_e/Q_e$  as the vertical axis and subjected to linear fitting. The values of  $Q_m$  and  $K_L$  were calculated with the slope and intercept of the fitted line, respectively [23].

##### 2.5.2. Freundlich isotherm equation

The Freundlich isotherm equation is based on multilayer adsorption and assumes that several

relationships exist between adsorbate and adsorbent. The general and linear expressions are, respectively, written as:

$$Q_e = K_F C_e^{1/n} \quad (9)$$

$$\ln Q_e = \ln K_F + \frac{1}{n} \ln C_e \quad (10)$$

where  $K_F$  represents the Freundlich constant ( $\text{mg/g}$ )<sup>1/ $n$</sup> , and  $n$  represents the adsorption intensity; i.e. the larger  $n$  is, the higher the adsorption performance. A curve was plotted with  $\ln C_e$  as the horizontal axis and  $\ln Q_e$  as the vertical and then subjected to linear fitting. The values of  $n$  and  $K_L$  were calculated from the slope and intercept of the fitted line, respectively [32].

### 2.5.3. Dubinin–Radushkevich equation

The D–R equation is written as:

$$\ln Q_e = \ln Q_m - \beta \varepsilon^2 \quad \varepsilon = RT \ln \left( 1 + \frac{1}{C_e} \right) \quad (11)$$

and

$$E = (2\beta)^{-1/2} \quad (12)$$

where  $R$  represents the thermodynamic constant,  $\beta$  represents the absorption energy constant ( $\text{kJ}^2/\text{mol}^2$ ),  $T$  represents the thermodynamic temperature (K),  $\varepsilon$  represents the Polanyi potential, and  $E$  represents the average adsorption free energy ( $\text{kJ/mol}$ ). A curve was plotted with  $\ln Q_e$  as the horizontal axis and  $\varepsilon^2$  as the vertical axis and subjected to linear fitting. The values of  $Q_m$  and  $\beta$  were calculated as the intercept and slope of the fitted line, respectively, and then  $E$  was obtained using Eq. (10) [33,34].

### 2.6. Orthogonal experimental design and analysis

Orthogonal experimental design and analysis are prevalently used for process optimization. Based on mathematical statistics, probability theory and practical experience, orthogonal experiments are designed using a standard orthogonal array. The experimental results are analyzed to determine the best design during the experimental design, the orthogonal array should be selected rationally and flexibly according to the actual levels and number of factors [35].

## 3. Results and discussion

### 3.1. Characterization of loofah sponge and AC

SEM images of loofah sponge and AC prepared from loofah sponge are shown in Fig. 1. The surfaces of both materials are rough and feature a highly porous structure, resulting in a high adsorption capacity. The determined BET surface area of loofah sponge is  $132.6 \text{ m}^2/\text{g}$  and that of AC is  $842.3 \text{ m}^2/\text{g}$ . These values reveal that the two adsorbents may have favorable adsorption properties.

FTIR analysis of loofah sponge allows spectrophotometric observation of the adsorbent surface in the wavenumber range of  $620\text{--}4,000 \text{ cm}^{-1}$ , providing a direct means to identify functional groups on the adsorbent surface. FTIR spectra of loofah sponge before and after adsorption are shown in Fig. 2(a). The FTIR spectra of loofah sponge before and after RhB adsorption were similar, possibly because of the low RhB adsorption ability of the loofah sponge. The characteristic peaks at  $3,338$  and  $1,592 \text{ cm}^{-1}$  were assigned to the stretching vibrations of the surface free hydroxyl groups (O–H), and that at  $2,897 \text{ cm}^{-1}$  was caused by the symmetric vibrations of C–H groups [36]. The peak at  $1,734 \text{ cm}^{-1}$  was ascribed to C=O stretching, while that at  $1,243 \text{ cm}^{-1}$  originated from C–H stretching vibrations. The intense peaks at  $1,000\text{--}1,500 \text{ cm}^{-1}$  are ascribed to the aromatic groups of lignin [37,38]. The positions of the bands at around  $800$  and  $3,500 \text{ cm}^{-1}$  did not change following RhB adsorption, indicating that RhB adsorption was a physical process rather than a chemical one [39].

FTIR spectra of AC in the wavenumber of  $400\text{--}4,000 \text{ cm}^{-1}$  before and after RhB adsorption are depicted in Fig. 2(b). The spectra revealed that there were different functional groups on the AC surface after RhB adsorption. The peak that emerged at  $2,921 \text{ cm}^{-1}$  can be assigned to the symmetric vibrations of C–H, which may be related to adsorption of RhB [40]. Many new peaks appeared at  $1,300\text{--}1,500 \text{ cm}^{-1}$  that may be caused by O–H groups and  $\text{CH}_2$  bending after RhB adsorption, indicating that the functional groups on the AC surface were covered or interacted with RhB. The peak at  $1,176 \text{ cm}^{-1}$  was ascribed to C–O–C stretching [36].

### 3.2. Effect of solution pH of RhB adsorption

Fig. 3(a) shows the effect of solution pH on the equilibrium adsorption of RhB by loofah sponge, revealing that pH strongly affected the removal ratio and equilibrium adsorption of RhB. Both the removal ratio and equilibrium adsorption of RhB were large at

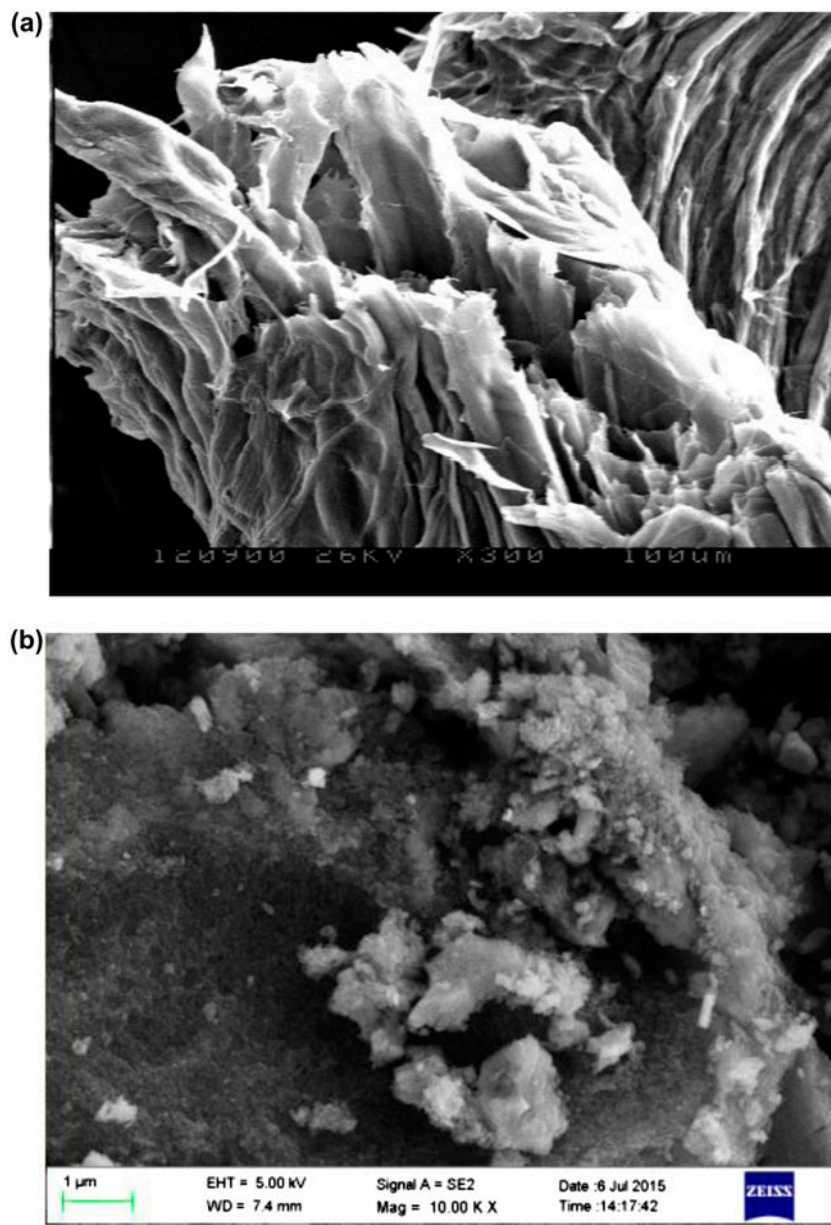


Fig. 1. SEM images of loofah before (a) and AC before (b) RhB adsorption.

pH 1. Therefore, the pH was adjusted to 1 for subsequent experiments. At very low pH (1.0), the surface of the adsorbent was highly protonated. In addition, at pH values lower than 3, RhB is present as a cationic monomer [41]. Thus, the RhB cations can easily enter the pore structure of the adsorbent at low pH. Above pH 3, the RhB removal ratio and adsorption capacity of loofah sponge decreased compared with those at lower pH. This is attributed to the zwitterionic form of RhB in water showing a tendency to aggregate, so it is unable to enter the pore structure of the adsorbent

[40]. Fig. 3(b) illustrates the effect of solution pH on equilibrium RhB adsorption by the AC prepared from loofah sponge. The influence of solution pH on the RhB removal ratio and equilibrium adsorption was very small. Therefore, pH was not adjusted in subsequent experiments using AC.

### 3.3. Effect of adsorbent content on RhB adsorption

The effect of loofah sponge content on RhB equilibrium adsorption and removal ratio is presented in

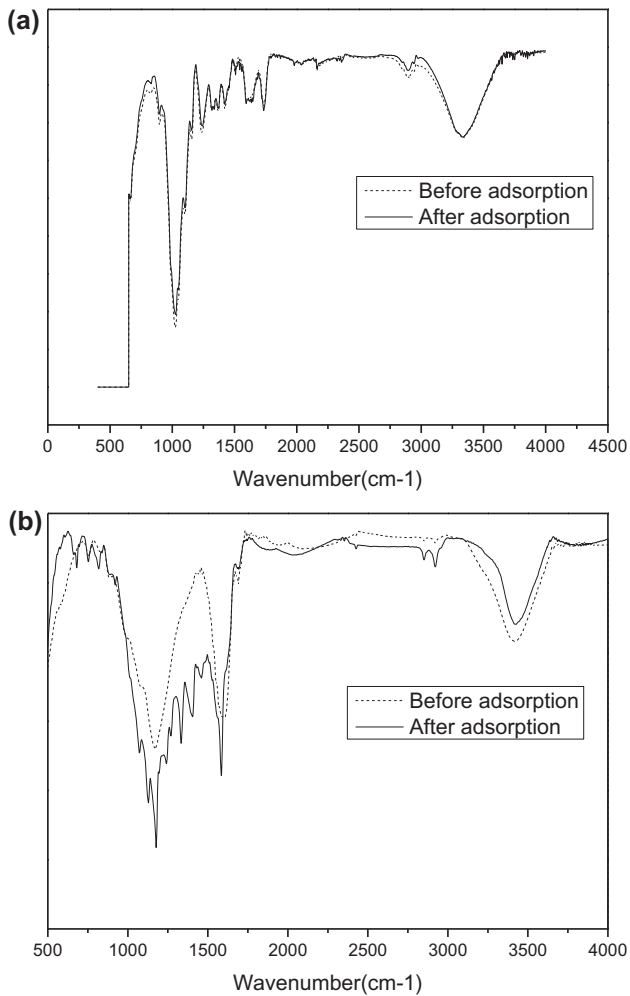


Fig. 2. FTIR spectra of loofah sponge (a) and AC (b) before and after adsorption of RhB.

Fig. 4(a). With increasing loofah sponge content, the removal ratio increased. The main reason for this is that a larger amount of loofah sponge increases the number of adsorption sites and dye adsorption capacity. Moreover, with increasing removal ratio, the equilibrium adsorption decreased. This is mainly because an increased loofah sponge content decreased the concentration of RhB, so some loofah pores were not saturated with RhB. Considering both removal ratio and efficient use of materials, the subsequent experiments used 2.0 g/L of loofah sponge.

As for the AC prepared from loofah sponge, the effects of its dosage on the RhB equilibrium adsorption and removal ratio are shown in Fig. 4(b). With increasing AC content, the RhB removal ratio increased while the equilibrium adsorption decreased gradually. The reason for the increase in RhB removal

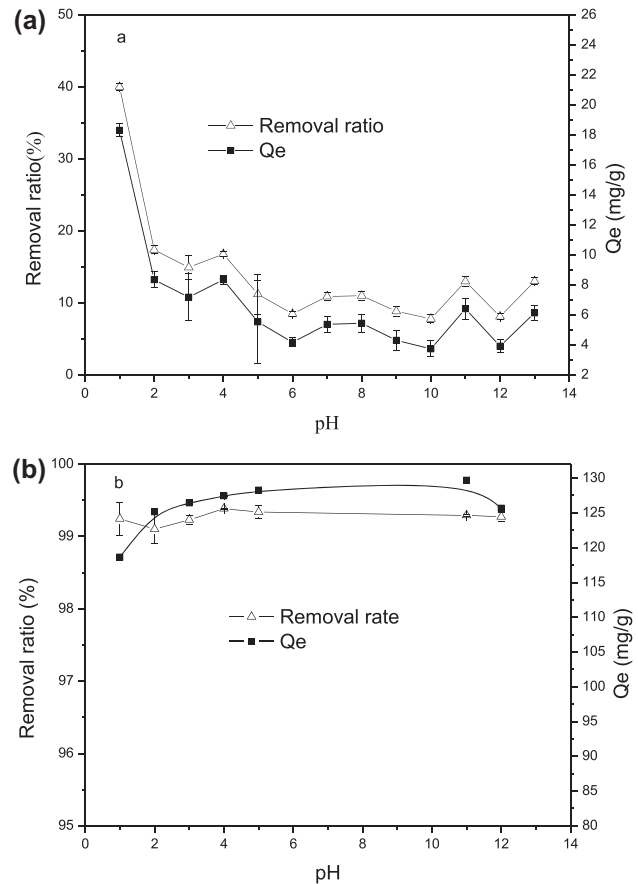


Fig. 3. Effect of pH on the removal ratio of RhB and adsorption capacity: (a) loofah sponge (loofah sponge content = 2.0 g/L,  $C_0 = 100$  mg/L,  $t = 180$  min, temperature = 298 K) and (b) AC (AC content = 0.8 g/L,  $C_0 = 100$  mg/L,  $t = 180$  min, temperature = 298 K).

ratio was the same as that of loofah described above, and again some sites failed to reach saturation at high AC content. In particular, when the RhB removal ratio approached 100%, further increasing the adsorbent amount no longer affected the removal ratio, but did lower the equilibrium adsorption. Therefore, the optimal content of AC was 0.8 g/L.

### 3.4. Effect of contact time and adsorption kinetics on RhB removal

Fig. 5(a) reveals that during RhB adsorption by loofah sponge, the RhB removal ratio increased with rising temperature. The effect of contact time of loofah sponge and AC on RhB removal ratio is illustrated in Fig. 5(b). With increasing adsorption time, the removal ratio of RhB increased gradually, and then reached equilibrium at 180 and 90 min for loofah sponge and

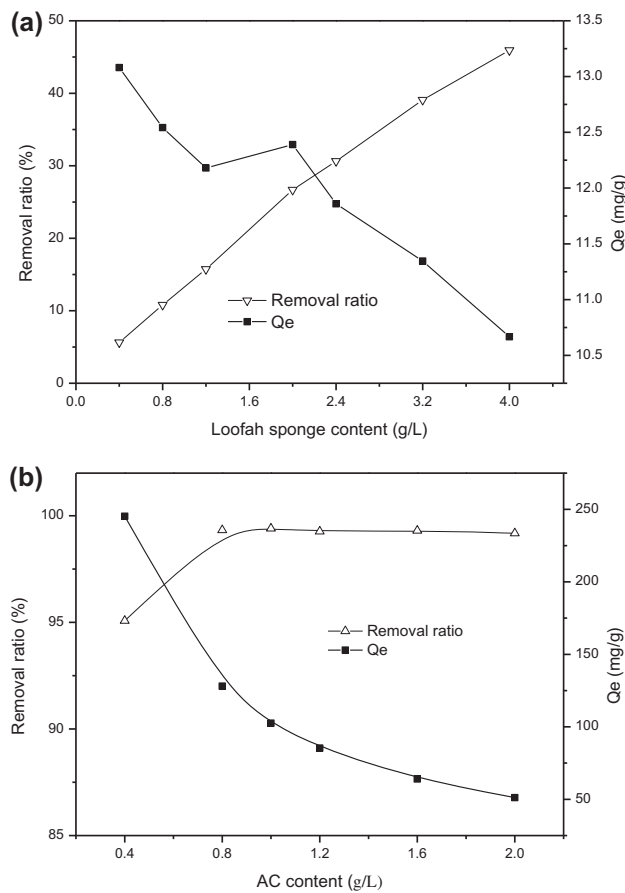


Fig. 4. Effect of adsorbent content on the removal ratio of RhB and adsorption capacity: (a) loofah sponge ( $C_0 = 100$  mg/L,  $t = 180$  min, temperature = 298 K) and (b) AC ( $C_0 = 100$  mg/L,  $t = 180$  min, temperature = 298 K).

AC, respectively. Therefore, the optimal equilibrium adsorption times of loofah sponge and AC for RhB were considered to be 180 and 90 min, respectively.

The kinetic simulation results for RhB adsorption by loofah sponge and AC are summarized in Table 1. The simulation results for both adsorbents reveal that they both had the largest correlation coefficient with respect to a pseudo-second-order equation, with correlation coefficients  $R^2$  of 0.9888 and 0.9999 for loofah sponge and AC at 298 K, respectively. Therefore, the kinetic models of these two adsorbents conform to pseudo-second-order equations. This indicates that the rate-limiting step of adsorption might be chemical sorption or chemisorption (including valence forces through the sharing or exchange of electrons) between adsorbate and adsorbent [42]. It has been reported that the RhB adsorption kinetics of a hyper-crosslinked polymeric adsorbent are pseudo-second-order [43].

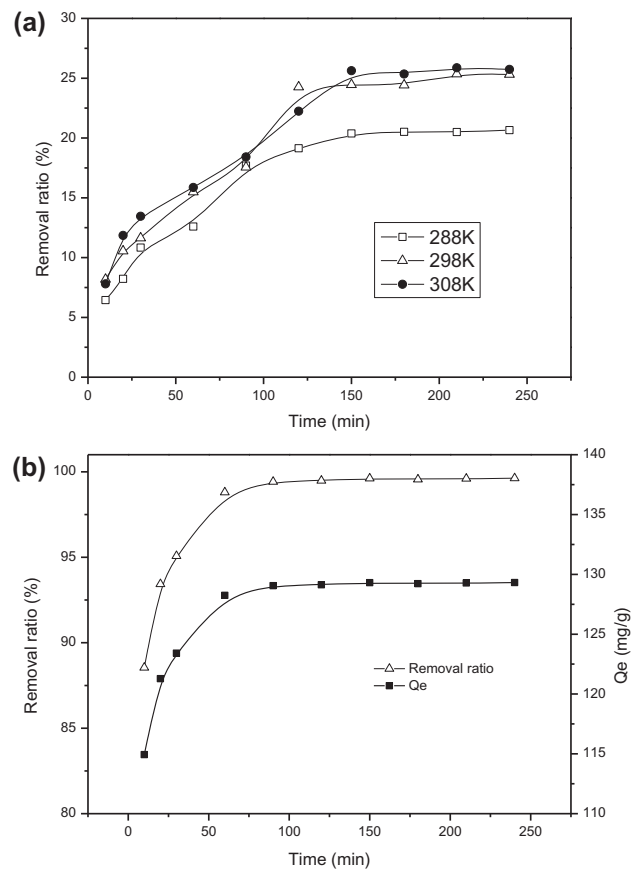


Fig. 5. Effect of contact time on the removal ratio of RhB and adsorption capacity: (a) loofah sponge at different temperatures (loofah sponge content = 2.0 g/L, pH 1,  $C_0 = 100$  mg/L, temperature = 298 K) and (b) AC (AC content = 0.8 g/L, pH 1,  $C_0 = 100$  mg/L, temperature = 298 K).

### 3.5. Adsorption isotherms

Adsorption isotherms are critical to evaluate the adsorption capacity of adsorbents and understand the nature of adsorbate–adsorbent interactions. The relationships between RhB equilibrium concentration and equilibrium adsorption of loofah sponge and AC are shown in Fig. 6. The equilibrium adsorption of RhB by loofah sponge was similar to the result of the Freundlich simulation, consistent with the largest  $R^2$  obtained for the Freundlich simulation of 0.9905, as indicated in Table 2. The experimental result for RhB equilibrium adsorption by AC was closest to that obtained from the Langmuir simulation;  $R^2$  of the Langmuir simulation the highest of the simulation models with a value of 0.9984. Therefore, the process of RhB adsorption by loofah sponge involves multilayer adsorption, while that of AC is monolayer adsorption, which occurs easily and quickly [44]. Furthermore, the maximum RhB adsorption capacity of

Table 1  
Kinetic parameters for the adsorption RhB on loofah sponge and AC at 298 K

Adsorbent	Pseudo-first-order equation			Pseudo-second-order equation			Particle diffusion equation				
	Experiment data $Q_e$ (mg/g)	$k_1$ ( $\text{min}^{-1}$ )	$Q_e$ ( $\text{mg g}^{-1}$ )	$R^2$	$k_2$ ( $\text{g mg}^{-1} \text{min}^{-1}$ )	$Q_e$ ( $\text{mg g}^{-1}$ )	$V_0$ ( $\text{mg g}^{-1} \text{min}^{-1}$ )	$R^2$	$k_p$ ( $\text{mg g}^{-1} \text{min}^{-1/2}$ )	$C$ ( $\text{mg g}^{-1}$ )	$R^2$
Loofah sponge	12.79	0.0193	12.19	0.96	$1.77 \times 10^{-3}$	14.64	0.38	0.9888	0.66	2.74	0.9097
AC	129.32	0.0315	9.97	0.8664	$6.59 \times 10^{-3}$	129.87	111.11	0.9999	0.86	117.82	0.6763

loofah sponge was 27.3 mg/g ( $R^2 = 0.9905$ ) and that of AC was 333.3 mg/g ( $R^2 = 0.9984$ ) at 298 K, as listed in Table 2. The adsorption capacities of the two samples are compared with those of other adsorbents in Table 3, which reveals that the loofah sponge has a high adsorption capacity for RhB compared with other materials [40,45–48].

3.6. Orthogonal experiment

Tables 4 and 5 present the results of orthogonal experiments for RhB adsorption by loofah sponge and AC, respectively. Because solution pH has little effect on RhB adsorption by AC, it was not considered as an influence factor for the AC group. An experimental design with three factors and three

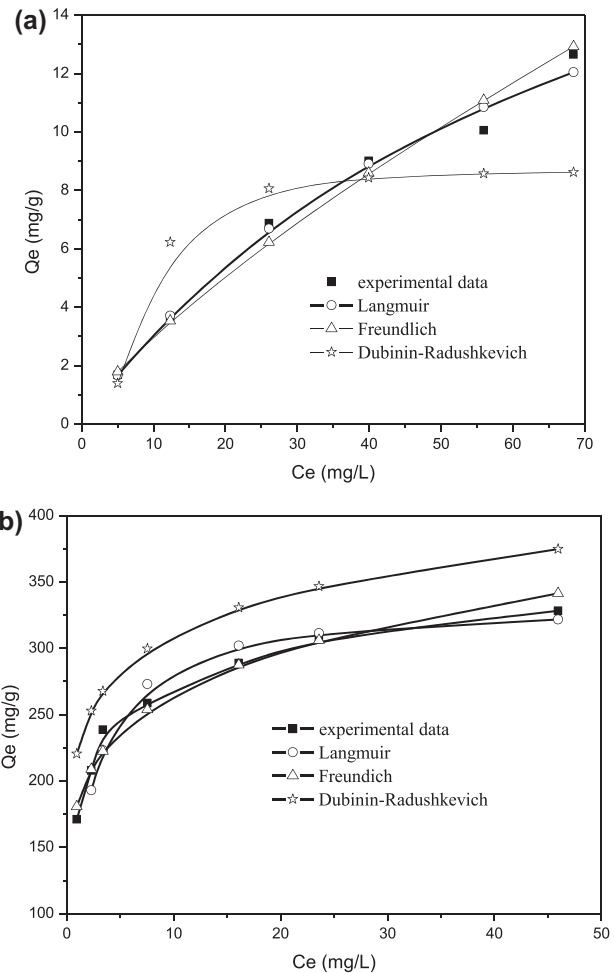


Fig. 6. Relationships between equilibrium concentration and equilibrium adsorption of RhB: (a) loofah sponge (loofah sponge content = 2.0 g/L, pH 1,  $t = 90$  min, temperature = 298 K) and (b) AC (AC content = 0.8 g/L, pH 1,  $t = 90$  min, temperature = 298 K).

Table 2

Parameters of the three adsorption isotherms for the adsorption of RhB on different adsorbents at 298 K

Adsorbent	Langmuir equation			Freundlich equation			Dubinin–Radushkevich equation			
	$Q_m$ (mg/g)	$K_L$ (L/mg)	$R^2$	$1/n$	$K_F$ (mg/g) <sup>1/n</sup>	$R^2$	$\beta$ (mol <sup>2</sup> /J <sup>2</sup> )	$Q_m$ (mg/g)	$E$ (kJ/mol)	$R^2$
Loofah sponge	23.70	0.0151	0.9552	0.7559	0.529	0.9905	$9.0 \times 10^{-6}$	8.72	0.236	0.8218
AC	333.33	0.6	0.9984	0.1639	182.29	0.9693	$1.0 \times 10^{-9}$	629.67	22.36	0.9814

Table 3

Comparison of maximum monolayer adsorption of RhB on various adsorbents

Adsorbents	Adsorption capacity (mg/g)	pH	$C_0$	Refs.
Sago waste carbon	16.2	5.7	16	[37]
Cellulose-based wastes	20.6	6–7	100	[41]
Parthenium biomass	59.2	7	250	[42]
Bagasse pith activated carbon	104	3.5	600	[43]
A-TRB	250	3.5	350	[44]
Loofah sponge	23.7	1	100	This work
Loofah sponge AC	333.3	Initial pH	100	This work

Table 4

The orthogonal experiment results of adsorption of RhB on loofah sponge

Test number	Test conditions and results					
	pH	Temperature (K)	Loofah sponge dosage (mg/L)	Concentration $C_0$ (mg/L)	Removal rate $\eta$ (%)	Equilibrium adsorption $Q_e$ (mg/g)
1	1	303	1.6	90	21.94	11.85
2	1	308	2.0	100	16.24	6.83
3	1	313	2.4	110	25.87	9.87
4	1.5	313	1.6	100	19.00	11.14
5	1.5	303	2.0	110	18.921	9.86
6	1.5	308	2.4	90	28.22	10.17
7	2	308	1.6	110	12.05	7.84
8	2	313	2.0	90	17.92	7.67
9	2	303	2.4	100	19.67	7.99

Table 5

The orthogonal experiment results of adsorption of RhB onto AC

Test number	Test conditions and results				
	Temperature (K)	Activated carbon dosage (mg/L)	Concentration $C_0$ (mg/L)	Removal rate $\eta$ (%)	Equilibrium adsorption $Q_e$ (mg/g)
1	313	0.6	120	99.20	191.43
2	313	0.8	100	99.46	126.71
3	313	1.0	80	99.11	82.28
4	308	0.6	80	99.40	136.93
5	308	0.8	120	99.40	144.62
6	308	1.0	100	99.52	101.73
7	318	0.6	100	99.48	163.31
8	318	0.8	80	99.57	102.28
9	318	1.0	120	99.43	101.64

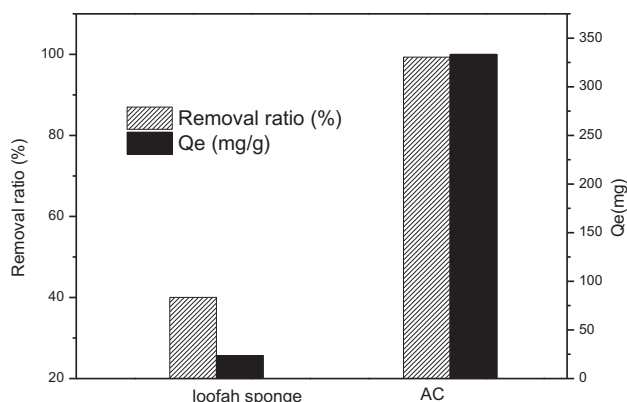


Fig. 7. Removal ratio and maximum equilibrium adsorption of RhB by loofah sponge and AC prepared from loofah sponge.

levels (nine trials) was designed. However, pH influenced RhB adsorption by loofah sponge. Therefore, nine trials with four factors and three levels were used for loofah sponge. Judging by the RhB removal ratio and equilibrium adsorption, the optimal adsorption effects of the two adsorbents were achieved through the following parameter combinations. For loofah sponge with the most effective adsorption (removal ratio of 28.22% and equilibrium adsorption of 10.17 mg/g), the optimal parameters were pH 1.5,  $T = 308$  K, loofah sponge content = 2.4 mg/L, and initial RhB concentration = 90 mg/L. For AC, the optimal performance (removal ratio of 99.20% and equilibrium adsorption of 191.43 mg/g) was achieved under the following conditions:  $T = 313$  K, AC content = 0.6 mg/L and initial RhB concentration = 120 mg/L.

### 3.7. Comparison of RhB removal ratio and maximum equilibrium adsorption of loofah sponge and AC

As shown in Fig. 7, the removal ratios of RhB by loofah sponge and AC reached 40.03 and 99.31%, respectively, and their maximum equilibrium adsorption reached 23.70 and 333.33 mg/g, respectively. In previous research, the maximum equilibrium adsorption of AC prepared from bagasse pith for removal of RhB from aqueous solution was only 198.6 mg/g [48]. After conversion into AC, the RhB adsorption performance of loofah sponge greatly increased; the maximum equilibrium adsorption increased by 13 times. The reason for this is that the AC prepared from loofah sponge had a high specific surface area of  $834 \text{ m}^2/\text{g}$ , which is 82 times that of loofah sponge ( $10.12 \text{ m}^2/\text{g}$ ) according to the surface area analysis. The AC had a typical hybrid microporous–mesoporous structure,

with a total pore volume of  $1.012 \text{ cm}^3/\text{g}$ . Thus makes AC derived from loofah sponge a good adsorbent, providing a new method for RhB removal from aqueous wastewater.

## 4. Conclusion

AC prepared from loofah sponge displayed an increased adsorption capacity for RhB compared with that of loofah sponge; the maximum equilibrium adsorption of AC reached  $333.33 \text{ mg/L}$ , 14 times that of loofah sponge. SEM analysis revealed that both samples had rough surfaces. Loofah sponge featured a high surface area of  $132.6 \text{ m}^2/\text{g}$  and AC had an even higher surface area of  $842.3 \text{ m}^2/\text{g}$ . FTIR analysis revealed the mechanism of RhB adsorption and amount of functional groups on the surface of the two materials, which may increase their adsorption capacity. The kinetic models for the adsorption process of loofah sponge and AC were consistent with pseudo-second-order equations. The adsorption isotherms showed that the adsorption process of loofah sponge involved multilayer adsorption, while that of AC was monolayer adsorption. The optimal performance of loofah sponge (removal ratio of 28.22% and equilibrium adsorption of 10.17 mg/g) was obtained when pH = 1.5,  $T = 308$  K, loofah sponge content = 2.4 mg/L, and initial RhB concentration = 90 mg/L. The optimal performance of AC (removal ratio of 99.20% and equilibrium adsorption of 191.43 mg/g) was achieved when  $T = 313$  K, AC content = 0.6 mg/L, and initial RhB concentration = 120 mg/L. AC derived from loofah sponge is a good adsorbent and displays promise as a new method to remove RhB from aqueous wastewater.

## Acknowledgments

This work was supported by a project funded by the Promotive Research Fund for Young and Middle-aged Scientists of Shandong Province (No. BS2014HZ019), projects of Shandong Province Higher Educational Science and Technology Program (Nos. J15LE07 and J15LH06), and the Major Science and Technology Program for Water Pollution Control and Treatment (No. 2012ZX07203004 and 2015ZX07203005).

## References

- [1] P.K. Mondal, R. Ahmad, S.Q. Usmani, Anaerobic biodegradation of triphenylmethane dyes in a hybrid UASFB reactor for wastewater remediation, *Biodegradation* 21 (2010) 1041–1047.

- [2] D. Tiwari, W. Kim, M. Kim, S.K. Prasad, S.-M. Lee, Organo-modified sericite in the remediation of phenol-contaminated waters, *Desalin. Water Treat.* 53 (2015) 446–451.
- [3] T.A. Khan, M. Nazir, E.A. Khan, Adsorptive removal of rhodamine B from textile wastewater using water chestnut (*Trapa natans* L.) peel: Adsorption dynamics and kinetic studies, *Toxicol. Environ. Chem.* 95 (2013) 919–931.
- [4] T.A. Khan, S. Dahiya, I. Ali, Use of kaolinite as adsorbent: Equilibrium, dynamics and thermodynamic studies on the adsorption of Rhodamine B from aqueous solution, *Appl. Clay Sci.* 69 (2012) 58–66.
- [5] T.A. Khan, S. Sharma, E.A. Khan, A.A. Mukhlif, Removal of congo red and basic violet 1 by chir pine (*Pinus roxburghii*) sawdust, a saw mill waste: Batch and column studies, *Toxicol. Environ. Chem.* 96 (2014) 555–568.
- [6] T.A. Khan, R. Rahman, I. Ali, E.A. Khan, A.A. Mukhlif, Removal of malachite green from aqueous solution using waste pea shells as low-cost adsorbent-adsorption isotherms and dynamics, *Toxicol. Environ. Chem.* 96 (2014) 569–578.
- [7] M. Anil Kumar, V. Vinoth Kumar, R. Ponnusamy, F. Paul Daniel, M. Seenivasan, D. Anuradha, S. Sivanesan, Concomitant mineralization and detoxification of acid red 88 by an indigenous acclimated mixed culture, *Environ. Prog. Sustainable Energy* 34 (2015) 1455–1466.
- [8] H. Mittal, S.B. Mishra, Gum ghatti and Fe<sub>3</sub>O<sub>4</sub> magnetic nanoparticles based nanocomposites for the effective adsorption of rhodamine B, *Carbohydr. Polym.* 101 (2014) 1255–1264.
- [9] S. Papic, N. Koprivanac, A.L. Božić, A. Meteš, Removal of some reactive dyes from synthetic wastewater by combined Al(III) coagulation/carbon adsorption process, *Dyes Pigm.* 62 (2004) 291–298.
- [10] N. Azbar, T. Yonar, K. Kestioglu, Comparison of various advanced oxidation processes and chemical treatment methods for COD and color removal from a polyester and acetate fiber dyeing effluent, *Chemosphere* 55 (2004) 35–43.
- [11] V. Golob, A. Vinder, M. Simonic, Efficiency of the coagulation/flocculation method for the treatment of dyebath effluents, *Dyes Pigm.* 67 (2005) 93–97.
- [12] M. Riera-Torres, C. Gutiérrez-Bouzán, M. Crespi, Combination of coagulation–flocculation and nanofiltration techniques for dye removal and water reuse in textile effluents, *Desalination* 252 (2010) 53–59.
- [13] I. Ali, S. Dahiya, K. Tabrez, Removal of direct red 81 dye from aqueous solution by native and citric acid modified bamboo sawdust—Kinetic study and equilibrium isotherm analyses, *Gazi Univ. J. Sci.* 25 (2012) 59–87.
- [14] T.A. Khan, M. Nazir, E.A. Khan, U. Riaz, Multiwalled carbon nanotube–polyurethane (MWCNT/PU) composite adsorbent for safranin T and Pb(II) removal from aqueous solution: Batch and fixed-bed studies, *J. Mol. Liq.* 212 (2015) 467–479.
- [15] V. Gupta, B. Gupta, A. Rastogi, S. Agarwal, A. Nayak, A comparative investigation on adsorption performances of mesoporous activated carbon prepared from waste rubber tire and activated carbon for a hazardous azo dye—Acid Blue 113, *J. Hazard. Mater.* 186 (2011) 891–901.
- [16] J. Zhang, Q. Shi, C. Zhang, J. Xu, B. Zhai, B. Zhang, Adsorption of Neutral Red onto Mn-impregnated activated carbons prepared from *Typha orientalis*, *Bioresour. Technol.* 99 (2008) 8974–8980.
- [17] J. Zhang, Y. Li, C. Zhang, Y. Jing, Adsorption of malachite green from aqueous solution onto carbon prepared from *Arundo donax* root, *J. Hazard. Mater.* 150 (2008) 774–782.
- [18] L. Wang, J. Zhang, R. Zhao, C. Li, Y. Li, C. Zhang, Adsorption of basic dyes on activated carbon prepared from *Polygonum orientale* Linn: Equilibrium, kinetic and thermodynamic studies, *Desalination* 254 (2010) 68–74.
- [19] L. Wang, J. Zhang, R. Zhao, Y. Li, C. Li, C. Zhang, Adsorption of Pb(II) on activated carbon prepared from *Polygonum orientale* Linn.: Kinetics, isotherms, pH, and ionic strength studies, *Bioresour. Technol.* 101 (2010) 5808–5814.
- [20] M.-S. Miao, Y.-N. Wang, Q. Kong, L. Shu, Adsorption kinetics and optimum conditions for Cr(VI) removal by activated carbon prepared from luffa sponge, *Desalin. Water Treat.* 57 (2016) 7763–7772.
- [21] L.B. Lim, N. Priyantha, N.H. Mohd Mansor, Utilizing *Artocarpus altilis* (breadfruit) skin for the removal of malachite green: Isotherm, kinetics, regeneration, and column studies, *Desalin. Water Treat.* 57 (2016) 16601–16610.
- [22] H.I. Chieng, L.B. Lim, N. Priyantha, Sorption characteristics of peat from Brunei Darussalam for the removal of rhodamine B dye from aqueous solution: Adsorption isotherms, thermodynamics, kinetics and regeneration studies, *Desalin. Water Treat.* 55 (2015) 664–677.
- [23] Q. Gao, H. Liu, C. Cheng, K. Li, J. Zhang, C. Zhang, Y. Li, Preparation and characterization of activated carbon from wool waste and the comparison of muffle furnace and microwave heating methods, *Powder Technol.* 249 (2013) 234–240.
- [24] I. Tan, B. Hameed, A. Ahmad, Equilibrium and kinetic studies on basic dye adsorption by oil palm fibre activated carbon, *Chem. Eng. J.* 127 (2007) 111–119.
- [25] P.S. Saudagar, N.S. Shaligram, R.S. Singhal, Immobilization of *Streptomyces clavuligerus* on loofah sponge for the production of clavulanic acid, *Bioresour. Technol.* 99 (2008) 2250–2253.
- [26] H. Liu, P. Dai, J. Zhang, C. Zhang, N. Bao, C. Cheng, L. Ren, Preparation and evaluation of activated carbons from lotus stalk with trimethyl phosphate and tributyl phosphate activation for lead removal, *Chem. Eng. J.* 228 (2013) 425–434.
- [27] X. Yang, C. Cao, L. Erickson, K. Hohn, R. Maghirang, K. Klabunde, Photo-catalytic degradation of Rhodamine B on C-, S-, N-, and Fe-doped TiO<sub>2</sub> under visible-light irradiation, *Appl. Catal. B: Environ.* 91 (2009) 657–662.
- [28] H. Liu, J. Zhang, W. Liu, N. Bao, C. Cheng, C. Zhang, Preparation and characterization of activated charcoals from a new source: Feather, *Mater. Lett.* 87 (2012) 17–19.
- [29] P. Yuan, M. Fan, D. Yang, H. He, D. Liu, A. Yuan, J. Zhu, T. Chen, Montmorillonite-supported magnetite nanoparticles for the removal of hexavalent chromium [Cr(VI)] from aqueous solutions, *J. Hazard. Mater.* 166 (2009) 821–829.

- [30] U. Isah, G. Abdurraheem, S. Bala, S. Muhammad, M. Abdullahi, Kinetics, equilibrium and thermodynamics studies of CI Reactive Blue 19 dye adsorption on coconut shell based activated carbon, *Int. Biodeterior. Biodegrad.* 102 (2015) 265–273.
- [31] Ö. Gerçel, A. Özcan, A.S. Özcan, H.F. Gerçel, Preparation of activated carbon from a renewable bio-plant of *Euphorbia rigida* by H<sub>2</sub>SO<sub>4</sub> activation and its adsorption behavior in aqueous solutions, *Appl. Surf. Sci.* 253 (2007) 4843–4852.
- [32] I. Tan, A. Ahmad, B. Hameed, Adsorption isotherms, kinetics, thermodynamics and desorption studies of 2, 4, 6-trichlorophenol on oil palm empty fruit bunch-based activated carbon, *J. Hazard. Mater.* 164 (2009) 473–482.
- [33] L. Ren, J. Zhang, Y. Li, C. Zhang, Preparation and evaluation of cattail fiber-based activated carbon for 2, 4-dichlorophenol and 2, 4, 6-trichlorophenol removal, *Chem. Eng. J.* 168 (2011) 553–561.
- [34] Q. Kong, Y.-N. Wang, L. Shu, M.-S. Miao, Isotherm, kinetic, and thermodynamic equations for cefalexin removal from liquids using activated carbon synthesized from loofah sponge, *Desalin. Water Treat.* 57 (2015) 7733–7742.
- [35] M.-S. Miao, Y.-N. Wang, Q. Kong, L. Shu, Adsorption kinetics and optimum conditions for Cr(VI) removal by activated carbon prepared from luffa sponge, *Desalin. Water Treat.* 57 (2016) 7763–7772.
- [36] V.O.A. Tanobe, T.H.D. Sydenstricker, M. Munaro, S.C. Amico, A comprehensive characterization of chemically treated Brazilian sponge-gourds (*Luffa cylindrica*), *Polym. Test.* 24 (2005) 474–482.
- [37] M. Ali, A. Emsley, H. Herman, R. Heywood, Spectroscopic studies of the ageing of cellulosic paper, *Polymer* 42 (2001) 2893–2900.
- [38] X. Colom, F. Carrasco, P. Pagès, J. Cañavate, Effects of different treatments on the interface of HDPE/lignocellulosic fiber composites, *Compos. Sci. Technol.* 63 (2003) 161–169.
- [39] G. Vijayakumar, R. Tamilarasan, M. Dharmendirakumar, Adsorption, Kinetic, Equilibrium and Thermodynamic studies on the removal of basic dye Rhodamine-B from aqueous solution by the use of natural adsorbent perlite, *J. Mater. Environ. Sci.* 3 (2012) 157–170.
- [40] J. Anandkumar, B. Mandal, Adsorption of chromium (VI) and Rhodamine B by surface modified tannery waste: Kinetic, mechanistic and thermodynamic studies, *J. Hazard. Mater.* 186 (2011) 1088–1096.
- [41] A.V. Deshpande, U. Kumar, Effect of method of preparation on photophysical properties of Rh-B impregnated sol-gel hosts, *J. Non-Cryst. Solids* 306 (2002) 149–159.
- [42] Y.-S. Ho, G. McKay, Pseudo-second order model for sorption processes, *Process Biochem.* 34 (1999) 451–465.
- [43] J.-H. Huang, K.-L. Huang, S.-Q. Liu, A.-T. Wang, C. Yan, Adsorption of Rhodamine B and methyl orange on a hypercrosslinked polymeric adsorbent in aqueous solution, *Colloids Surf., A* 330 (2008) 55–61.
- [44] W. Liu, J. Zhang, C. Cheng, G. Tian, C. Zhang, Ultrasonic-assisted sodium hypochlorite oxidation of activated carbons for enhanced removal of Co(II) from aqueous solutions, *Chem. Eng. J.* 175 (2011) 24–32.
- [45] K. Kadirvelu, C. Karthika, N. Vennilamani, S. Pattabhi, Activated carbon from industrial solid waste as an adsorbent for the removal of Rhodamine-B from aqueous solution: Kinetic and equilibrium studies, *Chemosphere* 60 (2005) 1009–1017.
- [46] G. Annadurai, R.-S. Juang, D.-J. Lee, Use of cellulose-based wastes for adsorption of dyes from aqueous solutions, *J. Hazard. Mater.* 92 (2002) 263–274.
- [47] J.-X. Yu, B.-H. Li, X.-M. Sun, J. Yuan, R.-A. Chi, Polymer modified biomass of baker's yeast for enhancement adsorption of methylene blue, rhodamine B and basic magenta, *J. Hazard. Mater.* 168 (2009) 1147–1154.
- [48] H.M. Gad, A.A. El-Sayed, Activated carbon from agricultural by-products for the removal of Rhodamine-B from aqueous solution, *J. Hazard. Mater.* 168 (2009) 1070–1081.